KJO
pISSN: 1011-8942 eISSN: 2092-9382

Korean J Ophthalmol 2022;36(4):318-325
https://doi.org/10.3341/kjo.2022.0012

Original Article

Impact of Lacrimal Gland Extraction on the Contralateral Eye in an Animal Model for Dry Eye Disease

Minha Kim[1], So Young Kim[2,3], Ji Won Jeon[1], Hyung Keun Lee[1,2]

[1]*Department of Ophthalmology, Institute of Vision Research, Yonsei University College of Medicine, Seoul, Korea*
[2]*Severance Institute for Vascular and Metabolic Research, Yonsei University College of Medicine, Seoul, Korea*
[3]*Institute of Biomedical Research, Yonsei University College of Medicine, Seoul, Korea*

Purpose: Although there is still no consensus on the best animal model for dry eye disease research, a model based on lacrimal gland extraction (LGE) model is widely used. In this study, we aimed to investigate the histopathological changes taking place on the contralateral eye after unilateral LGE to determine whether it is useful as a control.

Methods: Seven-week-old male C57BL/6 mice were divided into naive control, environmental chamber model, and LGE groups. Corneal fluorescein staining was scored to quantify the severity of damage. Morphological changes in the cornea, conjunctiva, and lacrimal gland (LG) were determined by hematoxylin and eosin staining and compared to those on naive control animals.

Results: Compared to naive subjects, the unilateral LGE model showed enhanced corneal erosion scores and loss of conjunctival goblet cells, not only on the ipsilateral but also on the contralateral side. These changes in the ocular surface became more pronounced in a time-dependent manner. Furthermore, loss of LG acinar cells and leukocyte infiltration were detected in the contralateral LGs of the LGE model.

Conclusions: Considering the changes observed in the ocular surface and LGs, the contralateral side of the LGE model may not offer proper control conditions for the experimental comparison of the effects of dry eye disease *in vivo*. There may be regulatory feedback or crosstalk system between both eyes activated in response to LGE.

Key Words: Animal models, Dry eye syndromes, Lacrimal gland

Dry eye (DE) is one of the most common diseases in the field of ophthalmology. The prevalence of DE disease (DED) has been reported to be between 5% and 34% depending on the country [1-3]. DED is considered to be a multifactorial disease that causes ocular discomfort, tear film instability and inflammation of the ocular surface [4-7]. Although it has been the focus of intense research, both clinical and based on *in vivo* experiments, the mechanism underlying DED (in particular, the non-Sjögren's type as well as Meibomian gland dysfunction) is not clearly understood yet [8,9].

Several murine *in vivo* models have been developed with the aim of uncovering the pathophysiology of DE and de-

Received: February 6, 2022 *Final revision:* April 19, 2022
Accepted: April 21, 2022

Corresponding Author: Hyung Keun Lee, MD, PhD. Department of Ophthalmology, Institute of Vision Research, Yonsei University College of Medicine, 50-1 Yonsei-ro, Seodaemun-gu, Seoul 03722, Korea. Tel: 82-2-2019-3440, Fax: 82-2-3463-1049, Email: shadik@yuhs.ac

termining the effectiveness of potential treatments, and they are currently being used to mimic clinical conditions for research purposes. These include a scopolamine injection model, a corneal erosion model, an environmental chamber model (ECM), a lacrimal gland extraction (LGE) model, and a knockdown model used specifically for research on Sjögren's syndrome [10-14]. Despite the profusion of animal models that have been developed, there is no standard *in vivo* model with wide consensus among researchers in the field, and it is therefore hard to compare the results from different studies directly. Moreover, significant variations in the results from different research groups have sometimes been observed, even when the same protocol was reportedly used.

The purpose of this study is twofold. The first is to compare ocular surface changes in response to a DE-inducing protocol between a LGE model, an ECM model, and a naive control group. The second is to determine whether changes on the ocular surface in the LGE model were also present on the contralateral side and compare them with those on the ipsilateral side.

Materials and Methods

Animals

Seven-week-old male C57BL/6 mice (Charles River Laboratory, Wilmington, MA, USA) were used as experimental subjects in accordance with the standards set forth in the Statement for the Use of Animals in Ophthalmic and Vision Research issued by the Association for Research in Vision and Ophthalmology. The research protocol was approved by the Institutional Animal Care and Use Committee of Yonsei University College of Medicine (No. YU-2015-0190). The *in vivo* experiments on mice were performed at the Institute of Vision Research of the Yonsei University College of Medicine. Twelve mice were randomly allocated to four different experimental groups (naive controls, ECM, ipsilateral LGE group, and contralateral LGE group), each composed of four individuals.

DE induction

DE was induced in the ECM group by placing the experimental subjects in a controlled environment chamber, which allows for the precise regulation and maintenance of ambient temperature (21°C–23°C), relative humidity (<30%), and airflow (15 L/min). To achieve maximum ocular surface dryness, the subjects were given subcutaneous injections of 0.1 mL scopolamine hydrobromide (5 mg/mL; Sigma-Aldrich, St. Louis, MO, USA) three times a day. On the subjects allocated to the ipsilateral and contralateral LGE groups, unilateral LGE was performed under general anesthesia. After making a V-shaped incision on the skin from the inferolateral side of the ear to the ramus of mandible, we dissected the subcutaneous tissue along the incision line, and this tissue together with the skin was flipped over. Then, the submandibular gland was located at the inferolateral side of the ear, with the lacrimal glands (LGs) and parotid glands very close to each other in front of it. They were separated along the fissure, and the extraorbital (main) LGs were removed and fixed with 100% methyl alcohol. The removed LGs were subsequently vacuum-dried and weighed.

Tissue preparation

At week 4, 5, and 6 after LGE, the mice were sacrificed. Tissue from the ocular surface, including the whole cornea with enough limbal area (containing minimal conjunctiva, approximately 0.3 mm from the corneal limbus) was cut from each eyeball (Fig. 1). The experiment was repeated three times with the same experimental settings.

Ocular surface examination

Clinical signs such as corneal erosion were assessed after fluorescein staining using a 1% fluorescein solution (Sigma-Aldrich) according to the standard National Eye Institute scoring system, as previously described [9]. Briefly, at the end of treatment, 1 mL of 1% fluorescein was applied to the lower conjunctival sac, and corneal fluorescein staining was examined using a slit-lamp biomicroscope after 3 minutes. Punctate staining was evaluated by an observer blinded to group allocation using the Oxford Scheme grading system, with each cornea receiving a grade between 0 and 5. Corneal erosion score (CES) was determined at week 5. To show more intuitive figures instead of blue light filter images with fluorescein dye, additional lissamine green dye was used. Lissamine green impregnated paper strips (Contacare Ophthalmics & Diagnostics, Padra,

India) were used.

Histological examination

The ocular surface tissue and the LGs were embedded in paraffin according to standard protocols. A microtome (Leica RM 2255; Leica Microsystems, Wetzlar, Germany) was used to slice the paraffin-embedded tissue blocks into 4 μm transverse sections that were placed on microscope slides. The slides were soaked in xylene for deparaffinization and then immersed in a graded series of ethanol solutions and in phosphate-buffered saline. After washing with

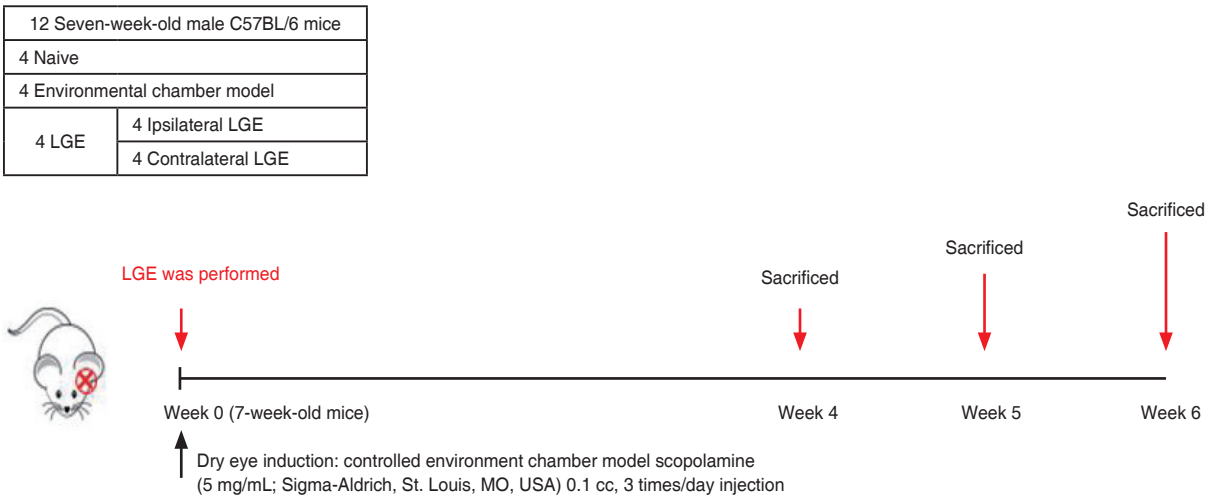

Fig. 1. Experimental timeline of tissue collection for the environmental chamber model and lacrimal gland extraction (LGE) models. At week 4, 5, and 6 after LGE, C57BL/6 mice (Charles River Laboratory, Wilmington, MA, USA) were sacrificed and eyeballs were collected. The experiment was repeated three times with the same experimental settings.

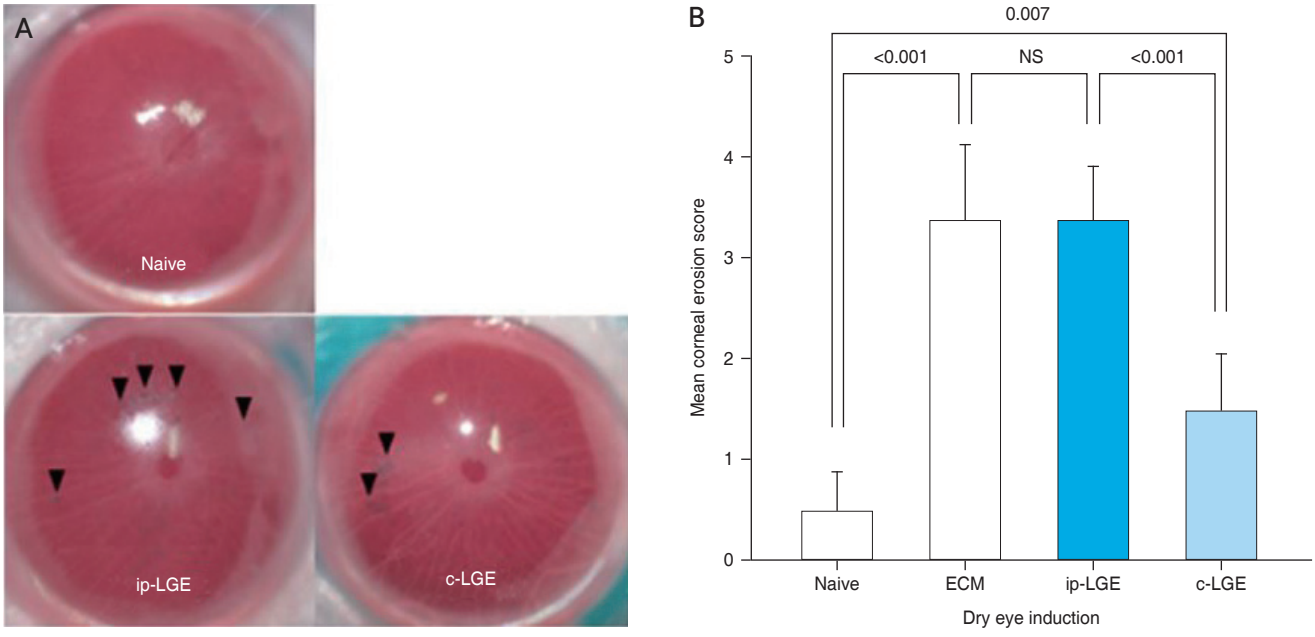

Fig. 2. Mean corneal fluorescein-stained erosion scores. (A) Representative images of the lissamine green-stained corneas from naive, ipsilateral lacrimal gland extraction (ip-LGE), and contralateral LGE (c-LGE) groups. Black arrowheads indicate corneal erosion. (B) Mean corneal erosion score measured 5 weeks after dry eye induction either by controlled environment chamber or LGE. ECM = environmental chamber model; NS = not significant.

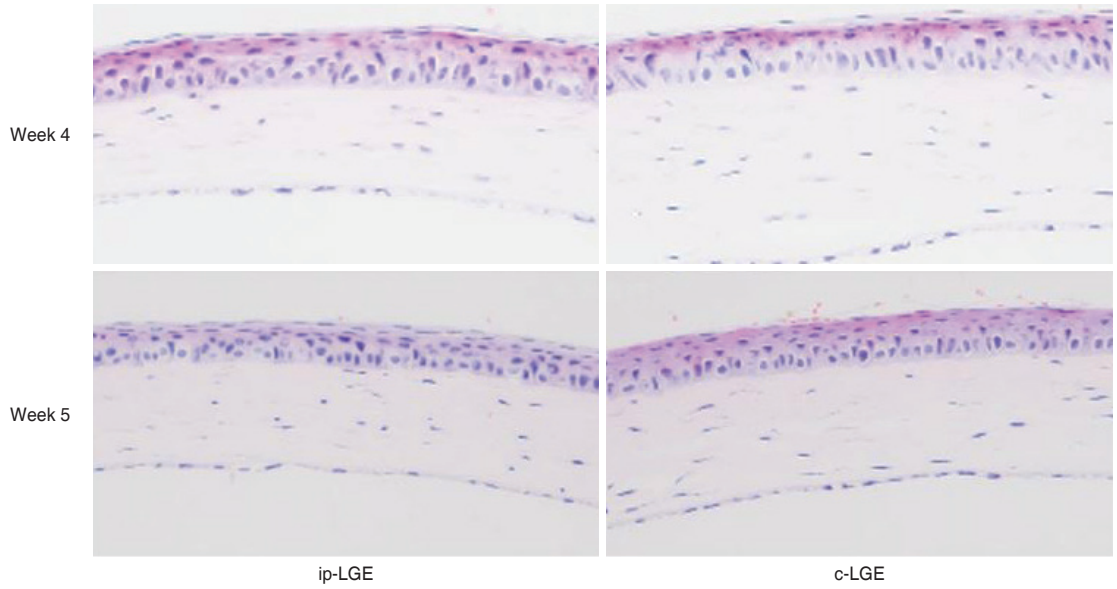

Fig. 3. Corneal histological differences between ipsilateral lacrimal gland extraction (ip-LGE) and contralateral LGE (c-LGE; H&E, ×200). Compared to 4 weeks after LGE, no sign of inflammation was observed in the enlarged bilateral corneal sections 5 weeks after LGE.

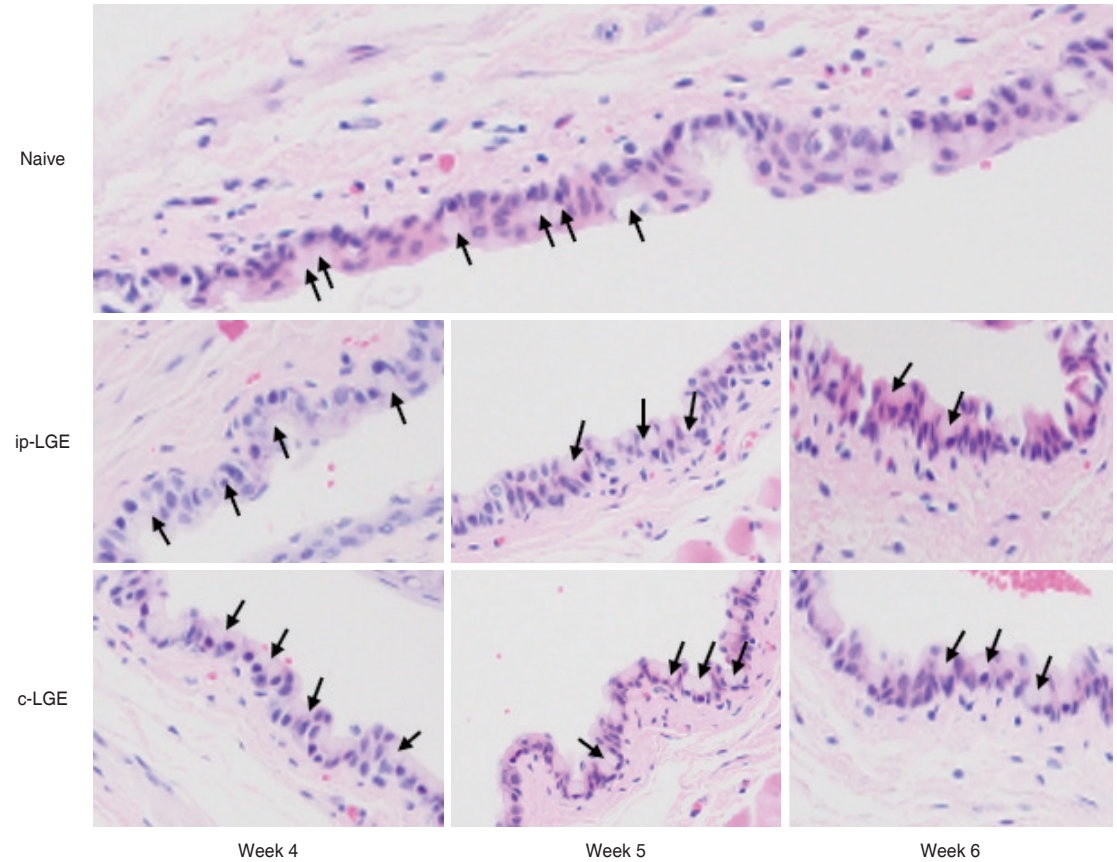

Fig. 4. Conjunctiva showing goblet cells within the epithelial layer (H&E, ×200). Loss of goblet cells and conjunctival flattening was noted on both ipsilateral lacrimal gland extraction (ip-LGE) and contralateral LGE (c-LGE) in the LGE group. The change was more prominent at 6 weeks after LGE. Black arrows indicate goblet cell.

phosphate-buffered saline, the transverse eyelid tissue sections were stained with hematoxylin and eosin (Sigma-Aldrich). Digital images of the eyelid tissue sections were recorded under light microscopy at ×200 magnification with an Olympus BX51 microscope and a DP72 camera (Olympus Corp., Tokyo, Japan) [15].

Statistical analysis

Statistical analyses were performed using IBM SPSS ver. 21.0 (IBM Corp., Armonk, NY, USA). One-way analysis of variance was used to make comparisons between three or more groups. A p-value equal or below 0.05 was considered significant. Results are presented as mean ± standard deviation.

Results

Differences in corneal fluorescein staining scores between the experimental groups

On week 5 of the study, the slit examination and scoring of the fluorescein-stained sections revealed a higher mean CES for the DE induction condition (Fig. 2A, 2B). The CES from the ECM group was significantly higher compared to the naive group ($p < 0.001$). As expected, the CES of ipsilateral LGE (ip-LGE) group was higher than that of the contralateral LGE (c-LGE) group ($p < 0.001$). Interestingly, the CES from the c-LGE group was also higher than that from the naive group ($p < 0.01$). There were no significant differences in score between the ECM and the ip-LGE groups ($p > 0.05$).

Comparison of histological changes in the ocular surface between the ip-LGE and c-LGE in the LGE model

As unilateral LGE resulted in an increased CES in the c-LGE group, histological changes in the cornea of the ip-LGE and the c-LGE groups were investigated. No significant differences in corneal morphology were detected on week 4 and 5 after LGE. In addition, the enlarged bilateral corneal section revealed no evident signs of inflammation, such as neutrophil infiltration into the corneal epithelium and stroma (Fig. 3). However, a gross appearance of decreased goblet cell density compared to the naive group was noted in the conjunctivas from the ip-LGE and c-LGE groups. A flattening of the conjunctival fold was also noted in both eyes. Interestingly, the loss of goblet cells and the flattening of the conjunctival fold in the c-LGE group were observed at a later time point compared to the ip-LGE group. These changes became more pronounced at 6 weeks after LGE (Fig. 4). However, there was no leukocyte infiltration into the conjunctiva.

Characterization of the changes in the contralateral LG after LGE

As we reported previously, the vascularity and size of the LGs is reduced in response to DE induction in an *in vivo* model [16-19]. Remarkably, changes in the contralateral LGs were also observed following unilateral LGE. The gross vascularity of the contralateral LGs at 6 weeks after

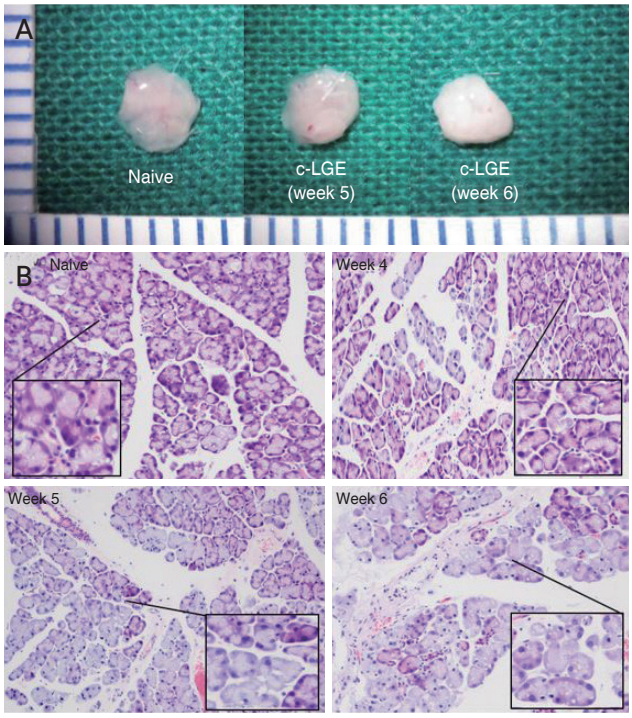

Fig. 5. Changes on the morphology and cellular composition in the contralateral lacrimal gland (LG; H&E, ×200). (A) Representative images of LG from a naive (control) mouse, and contralateral LG from a mouse allocated to the lacrimal gland extraction (LGE) group at 5 and 6 weeks postsurgery. The gross vascularity of the contralateral LGs at 6 weeks after LGE was prominently reduced and appeared paler compared to the naive condition. (B) Representative images of H&E-stained tissue from the contralateral LG. A widening of interlobular septa with infiltrating cells were found in the contralateral LG group in a time-dependent manner. c-LGE = contralateral lacrimal gland extraction.

LGE was prominently reduced and appeared paler, whiter, and with a condensed texture compared to the naive condition. Moreover, the LG size was reduced and correlated with the time elapsed since LGE (Fig. 5A). These changes were even more prominent on histological examination. Reduced acinar cell density in each lobule, and a widening of interlobular septa with infiltrating cells were found in the c-LG group in a time-dependent manner (Fig. 5B).

Discussion

The novel findings of our study include (1) a higher CES in the c-LGE compared to the naive group; and (2) an induction of conjunctival histological changes and pathologic changes in the LGs in the contralateral side in a model of unilateral LGE. All of these changes became more pronounced as time progressed.

In order to characterize histopathology changes caused by DE, we reestablished the DE induction period. In an animal model, Li et al. [20] and De Paiva et al. [21] used an induction period of up to 10 days, and Ikeda et al. [22] reported an induction of 2 weeks. Similarly, in most animal models for DE, the duration of DE induction is less than 2 weeks. However, when we designed this study, it was hypothesized that a longer induction period would increase the chances of detecting DE-related changes. This was based on the well-known relationship between age and DED [23,24]. In fact, several studies have used aged C57BL/6 mice as animal models [24], and our results show that all the DE-related changes become more pronounced with time, with a particularly noticeable change observed at 6 weeks after LGE.

Even the changes observed at 6 weeks after LGE can be described as mild compared to the disruption in the ocular surface typically observed in the course of DED [25]. The exact mechanism by which LGE induced the only mild ocular surface changes observed remains unknown, as we did not investigate it as part of our study. However, according to previous studies, infraorbital LGs as well as other minor glands have some compensatory role in the LGE model [26], which is absent in orbital LGs. In light of this, it is quite probable that complete absence of intraorbital and extraorbital LGs is needed to create a more reliable *in vivo* model, although such a model would still not mimic the clinical condition completely.

This study pays special attention to the changes taking place on the contralateral LGs. It can be inferred that regulatory feedback or crosstalk system may exist between both eyes [27-36]. However, as in the previous case, the exact mechanism underlying these changes is not known, and the involvement of the neurotransmitter or centripetal stimulation of the trigeminal nerve can only be hypothesized. This kind of neural control is also observed in other diseases. For instance, a previous study that focused on a unilateral disease (herpes zoster ophthalmicus) found a significant bilateral loss of limbal stem cells and subbasal nerve plexus compared to normal subjects [37,38].

There are several limitations in the present study. Firstly, it was a small sized, observational study, and it characterized changes in the LGs in different mice at certain time intervals instead of evaluating serial tissue sections obtained from the same eye. This study was conducted three times with the same settings, and we could get similar histopathology results. Nevertheless, the small number of subjects is a limitation of our study. Secondly, our study showed many representative images, but there are required to be more discernible and appropriate. For example, if a blue light filter image with fluorescein dye was obtained, the readers could differentiate CES more easily from the presented figures. Lastly, the pathological mechanisms underlying the changes of the ocular surface in the contralateral side were not investigated. Therefore, further studies on humans and on murine models are essential for uncovering them.

In conclusion, although no animal model completely recapitulates the pathological changes observed in humans affected by DED, the LGE model is potentially valuable for DE research, as it may mimic the condition of severe damage to the LGs observed in humans. However, as evidenced by the changes in the contralateral side that this model demonstrated in the present study, we believe it is worth pointing out that the contralateral side is not suitable as a proper control condition in experiments with DED models. Finally, the most appropriate murine model capable of mimicking the pathology of non-Sjögren's type DE remains to be determined.

Conflicts of Interest: Hyung Keun Lee(Corresponding Author) has been an Editorial board of the *Korean Journal of Ophthalmology* since 2015. However, he was not involved in the peer reviewer selection, evaluation, or deci-

sion process of this article. Otherwise, no other potential conflicts of interest relevant to this article were reported.

Acknowledgements: None.

Funding: None.

References

1. Hantera MM. Trends in dry eye disease management worldwide. *Clin Ophthalmol* 2021;15:165-73.
2. Alkabbani S, Jeyaseelan L, Rao AP, et al. The prevalence, severity, and risk factors for dry eye disease in Dubai: a cross sectional study. *BMC Ophthalmol* 2021;21:219.
3. Shanti Y, Shehada R, Bakkar MM, Qaddumi J. Prevalence and associated risk factors of dry eye disease in 16 northern West bank towns in Palestine: a cross-sectional study. *BMC Ophthalmol* 2020;20:26.
4. Ji YW, Mittal SK, Hwang HS, et al. Lacrimal gland-derived IL-22 regulates IL-17-mediated ocular mucosal inflammation. *Mucosal Immunol* 2017;10:1202-10.
5. Lee HK, Kim KW, Ryu JS, et al. Bilateral effect of the unilateral corneal nerve cut on both ocular surface and lacrimal gland. *Invest Ophthalmol Vis Sci* 2019;60:430-41.
6. Ji YW, Lee JH, Choi EY, et al. HIF1α-mediated TRAIL expression regulates lacrimal gland inflammation in dry eye disease. *Invest Ophthalmol Vis Sci* 2020;61:3.
7. Zoukhri D. Effect of inflammation on lacrimal gland function. *Exp Eye Res* 2006;82:885-98.
8. Schrader S, Mircheff AK, Geerling G. Animal models of dry eye. *Dev Ophthalmol* 2008;41:298-312.
9. Bron AJ. Diagnosis of dry eye. *Surv Ophthalmol* 2001;45 Suppl 2:S221-6.
10. Stern ME, Pflugfelder SC. What we have learned from animal models of dry eye. *Int Ophthalmol Clin* 2017;57:109-18.
11. Lio CT, Dhanda SK, Bose T. Cluster analysis of dry eye disease models based on immune cell parameters: new insight into therapeutic perspective. *Front Immunol* 2020;11:1930.
12. Willcox M, Argueso P, Georgiev GA, et al. TFOS DEWS II tear film report. *Ocul Surf* 2017;15:366-403.
13. Bron AJ, de Paiva CS, Chauhan SK, et al. TFOS DEWS II pathophysiology report. *Ocul Surf* 2017;15:438-510.
14. Novack GD, Asbell P, Barabino S, et al. TFOS DEWS II clinical trial design report. *Ocul Surf* 2017;15:629-49.
15. Eom Y, Han JY, Kang B, et al. Meibomian glands and ocular surface changes after closure of meibomian gland orifices in rabbits. *Cornea* 2018;37:218-26.
16. Xiao B, Wang Y, Reinach PS, et al. Dynamic ocular surface and lacrimal gland changes induced in experimental murine dry eye. *PLoS One* 2015;10:e0115333.
17. Kong L, Robinson CP, Peck AB, et al. Inappropriate apoptosis of salivary and lacrimal gland epithelium of immunodeficient NOD-scid mice. *Clin Exp Rheumatol* 1998;16:675-81.
18. Seo Y, Ji YW, Lee SM, et al. Activation of HIF-1α (hypoxia inducible factor-1α) prevents dry eye-induced acinar cell death in the lacrimal gland. *Cell Death Dis* 2014;5:e1309.
19. Ji YW, Kang HG, Song JS, et al. The dopaminergic neuronal system regulates the inflammatory status of mouse lacrimal glands in dry eye disease. *Invest Ophthalmol Vis Sci* 2021;62:14.
20. Li Z, Choi W, Oh HJ, Yoon KC. Effectiveness of topical infliximab in a mouse model of experimental dry eye. *Cornea* 2012;31 Suppl 1:S25-31.
21. De Paiva CS, Villarreal AL, Corrales RM, et al. Dry eye-induced conjunctival epithelial squamous metaplasia is modulated by interferon-gamma. *Invest Ophthalmol Vis Sci* 2007;48:2553-60.
22. Ikeda K, Simsek C, Kojima T, et al. The effects of 3% diquafosol sodium eye drop application on meibomian gland and ocular surface alterations in the Cu, Zn-superoxide dismutase-1 (Sod1) knockout mice. *Graefes Arch Clin Exp Ophthalmol* 2018;256:739-50.
23. de Paiva CS. Effects of aging in dry eye. *Int Ophthalmol Clin* 2017;57:47-64.
24. McClellan AJ, Volpe EA, Zhang X, et al. Ocular surface disease and dacryoadenitis in aging C57BL/6 mice. *Am J Pathol* 2014;184:631-43.
25. Chang YA, Wu YY, Lin CT, et al. Animal models of dry eye: their strengths and limitations for studying human dry eye disease. *J Chin Med Assoc* 2021;84:459-64.
26. Maitchouk DY, Beuerman RW, Ohta T, et al. Tear production after unilateral removal of the main lacrimal gland in squirrel monkeys. *Arch Ophthalmol* 2000;118:246-52.
27. Muller LJ, Marfurt CF, Kruse F, Tervo TM. Corneal nerves: structure, contents and function. *Exp Eye Res* 2003;76:521-42.
28. Tuominen IS, Konttinen YT, Vesaluoma MH, et al. Corneal innervation and morphology in primary Sjögren's syndrome. *Invest Ophthalmol Vis Sci* 2003;44:2545-9.
29. Roda M, Corazza I, Bacchi Reggiani ML, et al. Dry eye disease and tear cytokine levels: a meta-analysis. *Int J Mol Sci* 2020;21:3111.
30. Belmonte C, Acosta MC, Gallar J. Neural basis of sensation

in intact and injured corneas. *Exp Eye Res* 2004;78:513-25.

31. Sibony PA, Walcott B, McKeon C, Jakobiec FA. Vasoactive intestinal polypeptide and the innervation of the human lacrimal gland. *Arch Ophthalmol* 1988;106:1085-8.
32. Dartt DA. Regulation of tear secretion. *Adv Exp Med Biol* 1994;350:1-9.
33. Dartt DA. Neural regulation of lacrimal gland secretory processes: relevance in dry eye diseases. *Prog Retin Eye Res* 2009;28:155-77.
34. Botelho SY, Hisada M, Fuenmayor N. Functional innervation of the lacrimal gland in the cat. Origin of secretomotor fibers in the lacrimal nerve. *Arch Ophthalmol* 1966;76:581-8.
35. Botelho SY. Tears and the lacrimal gland. *Sci Am* 1964; 211:78-86.
36. Yamaguchi T, Hamrah P, Shimazaki J. Bilateral alterations in corneal nerves, dendritic cells, and tear cytokine levels in ocular surface disease. *Cornea* 2016;35 Suppl 1(Suppl 1): S65-70.
37. Liu X, Xu S, Wang Y, et al. Bilateral limbal stem cell alterations in patients with unilateral herpes simplex keratitis and herpes zoster ophthalmicus as shown by in vivo confocal microscopy. *Invest Ophthalmol Vis Sci* 2021;62:12.
38. Hamrah P, Cruzat A, Dastjerdi MH, et al. Corneal sensation and subbasal nerve alterations in patients with herpes simplex keratitis: an in vivo confocal microscopy study. *Ophthalmology* 2010;117:1930-6.